Journal of Electronics and Electrical Engineering
https://ojs.wiserpub.com/index.php/JEEE

Research Article

A Novel Static Model in d-q Coordinates for a Common-Emitter Amplifier

José M. Campos-Salazar[1*], Roya Rafiezadeh[2]

[1] Electronic Engineering Department, Universitat Politècnica de Catalunya, Barcelona, Spain
[2] Power Electronics and Machine Centre, University of Nottingham, Nottingham, United Kingdom
E-mail: jose.manuel.campos@upc.edu

Received: 25 May 2024; **Revised:** 2 September 2024; **Accepted:** 23 September 2024

Abstract: This work presents a comprehensive investigation into a novel static model, formulated in d-q coordinates, for a common-emitter amplifier operating in a common-emitter configuration. The research starts with an in-depth study of the standard dc and ac models of the common-emitter amplifier, elucidating essential equations that capture its linear behavior. Moreover, the focus shifts towards a small-signal model, specially adapted to the ac operation of the common-emitter amplifier. Park's transformation is utilized to derive a static model in d-q coordinates, offering a thorough representation of the amplifier's behavior under steady-state conditions. Simulation techniques are employed to rigorously evaluate and compare the proposed d-q coordinate model with the standard model. The study demonstrates the static and fast response capabilities of the derived d-q coordinate model after system start-up, thus proving its viability and effectiveness. This research presents valuable contributions to the field of common-emitter amplifier modeling and analysis, offering insights that can advance the design and comprehension of amplification systems.

Keywords: common-emitter amplifier, static model, d-q coordinates, Clarke transform, Park transform, amplifier modeling

1. Introduction

The theory of low-power signal amplification is a prominent topic in the field of microelectronics, highlighting significant research interest [1, 2, 3, 4, 5, 6, 7, 8, 9, 10, 11, 12, 13, 14, 15]. Among the commonly used devices for amplification in this domain are bipolar junction transistors (BJTs) and operational amplifiers (OP-Amps) [1, 2, 3, 4, 5, 6, 7, 8, 9, 10, 11, 12, 13, 14, 15]. On the other hand, field-effect transistors (JFETs and MOSFETs) find primary utility in switching applications [16] and are less prevalent in amplifier setups. OP-Amps have gained considerable prominence for amplifier applications across a broad frequency spectrum, whereas the use of BJTs for amplification purposes has declined, except in power amplifier applications [17, 18]. For medium-frequency voltage amplification, OP-Amps have become the preferred choice [17, 18]. However, in such applications, the amplification mechanisms are not regulated and rely on resistors in the bias circuit [17, 18]. This differs from amplifiers based on BJTs, where the gain expression is directly influenced by the load resistor, leading to complications in regulating the output voltage due to potential disturbances in the load resistor.

To address the drawback of gain dependence on the load resistor, a fundamental concept from control theory is introduced here. By incorporating a feedback loop that compares the output voltage with a reference value, an error signal

DOI: https://doi.org/10.37256/jeee.3220245024

is generated. This error signal is then fed to a controller or compensator, which produces a signal to drive the actuator of the amplifier [19, 20]. The challenge lies in determining the appropriate actuator and compensator to achieve the desired operation of the amplifier. However, due to the sinusoidal nature of the waveforms with which the amplifiers operate, their output dynamics—in particular the output voltages—remain sinusoidal even in steady-state conditions. This sinusoidal behavior provides a challenge for the use of linear compensators, even when the amplifier models themselves are linear in nature [19, 20, 21]. To overcome this limitation, a viable solution is to derive an amplifier model with static dynamics. This provides a model from which a linear compensator can be designed.

This work introduces a novel model of an amplifier in the common-emitter configuration utilizing variables with static dynamics, represented in d-q coordinates. The transformation process involves converting the original system, initially described in sinusoidal coordinates, into an α-β rotational coordinate system using the Clarke transform. Subsequently, the Park transform is applied to this rotating system, resulting in a static system represented in d-q coordinates, which are situated within a rotating reference frame [22]. This approach allows for a comprehensive understanding and analysis of the common-emitter amplifier's behavior in steady-state conditions.

This article presents a proof of concept demonstrating the applicability of modern control theory in the context of a dynamic model expressed in d-q coordinates. The application of control laws, such as state feedback controllers or classical control laws as feedback output compensators, is demonstrated to be a viable approach. While this work does not establish the foundations for synthesizing these control laws, it highlights the advantages of a static model as a function of time [23].

To validate the accuracy and proper functioning of the d-q model, an inverse transformation is applied to convert the d-q model back to the standard model. This process allows for a comparison of variables between the original standard model and the reconverted model. By evaluating the correlation between these variables, the suitability of the derived model can be determined. Furthermore, both the standard model and the model in d-q coordinates are subjected to simulations to evaluate and confirm the reliability of the proposed model. Through these simulations, the performance and behavior of the common-emitter amplifier can be thoroughly analyzed and compared in different scenarios and operating conditions.

Taking into account these verification steps, the paper ensures the proper functioning of the d-q model and establishes its practicality and effectiveness, making it a significant contribution to the field of common-emitter amplifier modeling and analysis. The paper is organized as follows: Section 1 introduces the problem and the motivation of the proposal. Sections 2 and 3 introduce the common-emitter amplifier topology and present the modeling of the common-emitter amplifier in both direct current and alternating current regimes, respectively. Section 4 is the core of the paper and introduces the proposed model in d-q coordinates. Sections 5 and 6 show the modeling of the common-amplifier in d-q coordinates and the solution of the dynamic equation. Finally, Sections 7 and 8 present the dynamic equation solution and conclusion, respectively.

2. Common-emitter amplifier topology

The topology of the CEA is depicted in Figure 1. This configuration is the most common within the transistor amplifier family [24]. In this circuit the BJT is represented by Q_1. The topology also shows the bias resistors R_1 and R_2, the collector resistor R_C and the emitter resistor R_E. The bias voltage is defined as V_{CC}. In the ac operating regime, the C_C coupling capacitor connects to the circuit, the input stage, configured by a sinusoidal voltage source $v_i(t)$ and an inductor L operating as an input filter. The coupling capacitor C_B allows to connect the CEA with the output stage comprised by a capacitor C operating as an output filter and the load resistor R_L. The currents $i_i(t)$, $i_C(t)$, $i_B(t)$, and $i_E(t)$ are the input, collector, base, and emitter currents, respectively. The voltages $v_{BE}(t)$ and $v_{CE}(t)$ are the voltages measured between the base and emitter and between collector and emitter, respectively. Finally, $v_o(t)$ and $v_C(t)$ are the output and capacitor voltages, respectively. Also, $v_o(t) = v_C(t)$ is verified.

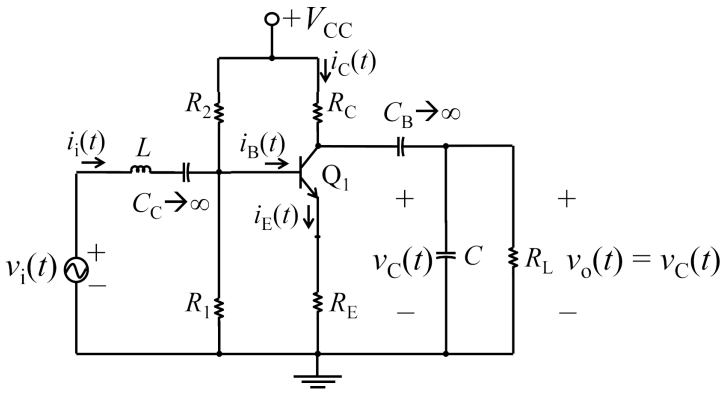

Figure 1. CEA topology

3. Common-emitter amplifier modeling

In this section, the fundamental equations governing the CEA are derived, taking into account both the dc and ac operating conditions. It is assumed that transistor Q_1 operates in the linear region, ensuring accurate signal amplification [17, 18].

3.1 *dc operation*

During dc operation, the coupling capacitors (C_B and C_C) behave as open circuits, leading to a modified circuit configuration depicted in Figure 2a, commonly known as a dc biased CEA [17, 18]. By combining resistors R_1, R_2, and the voltage source V_{CC}, a Thévenin equivalent circuit can be derived, resulting in a new CEA circuit specifically designed for the dc regime, as illustrated in Figure 2b. It should be noted that in Figure 2, lowercase letters are replaced with uppercase letters, as it is assumed that the variables represent solely dc components. The definitions of V_{BB} and R_B, are defined as follows

$$V_{BB} = \frac{R_B}{R_2} \cdot V_{CC} \tag{1}$$

$$R_B = R_1 || R_2 \tag{2}$$

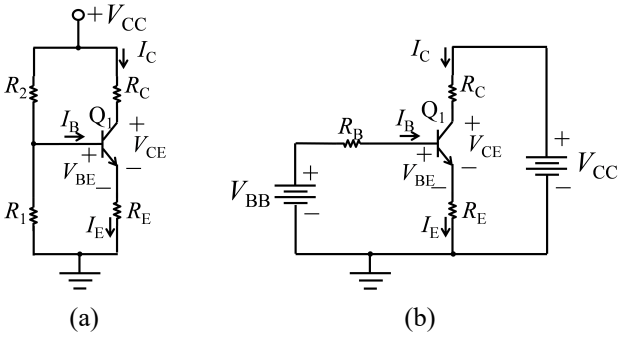

Figure 2. CEA operating in dc regime. (**a**) Topology in dc bias. The capacitors C_B and C_C act as open circuits. (**b**) Topology in dc bias with equivalent Thévenin input network

Considering (1) and (2), the information provided in Figure 2b and references [17, 18], the operating point of the CEA can be determined to achieve a maximum voltage output excursion, $v_o(t)$.

This operating point is defined as

$$V_{CE_Q} = \frac{1}{2} \cdot V_{CC} \tag{3}$$

$$I_{C_Q} = \frac{V_{BB} - V_{BE}}{\frac{R_B}{\beta} + R_E} \tag{4}$$

Equation (4) indicates that βrepresents the amplification factor in dc [17]. As the assumption is made that Q_1 operates within the linear region, the expressions $I_{CQ} = \beta \cdot I_B$, $I_{EQ} \approx I_{CQ}$, and $V_{BE} = V_\gamma = 0.7$ V can be verified.

3.2 *ac operation*

During ac operation of the CEA, the capacitors C_C and C_B are considered short circuits and the source V_{CC} is short circuited. In addition, Q_1 is replaced with its small-signal model [17, 18], assuming it operates in the linear region and $v_i(t)$ operates at high frequency. The small-signal model of the CEA is illustrated in Figure 3. It should be noted that the distinctions in modeling C_C and C_B as short circuits in Figure 3 are deliberate and based on their respective roles and frequency-dependent behaviors within the circuit. Capacitors C_C and C_B facilitate the path of the high-frequency sinusoidal input by behaving as short circuits, while inductor L serves its filtering purpose by acting as an open circuit at the same frequency. Capacitor C's behavior is determined by its specific filtering role within the circuit design.

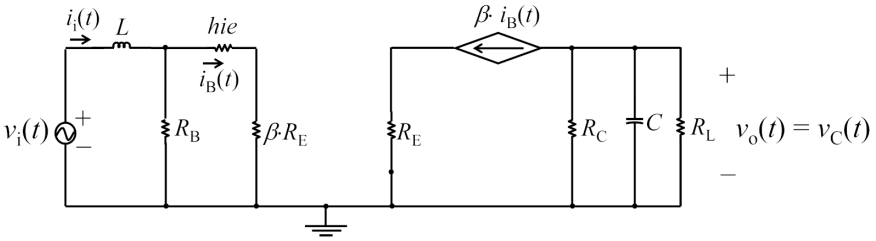

Figure 3. Small-signal model of the CEA

The small-signal model shown in Figure 3 is derived and defined and given by

$$\begin{cases} \dot{\mathbf{x}}(t) = \mathbf{A} \cdot \mathbf{x}(t) + \mathbf{B} \cdot u(t) \\ \mathbf{y}(t) = \mathbf{C} \cdot \mathbf{x}(t) + \mathbf{D} \cdot u(t) \end{cases} \tag{5}$$

In this model, the input is scalar and defined as $u(t) = v_i(t)$. On the other hand, the state vector is defined as $\mathbf{x}(t) = [i_i(t), v_o(t)]^T$. Moreover, in this case the output vector is defined as $\mathbf{y}(t) = \mathbf{x}(t)$.

Symbolically, $\{\mathbf{x}(t), \mathbf{y}(t)\} \in \{\mathbb{R}^2\}$. The model matrices are defined as follows:

$$\mathbf{A} = \begin{bmatrix} -\frac{R_i}{L} & 0 \\ -\frac{k}{C} & -\frac{1}{R_o \cdot C} \end{bmatrix} \quad \mathbf{B} = \begin{bmatrix} \frac{1}{L} \\ 0 \end{bmatrix}$$
$$\mathbf{C} = \begin{bmatrix} 1 & 0 \\ 0 & 1 \end{bmatrix} \quad \mathbf{D} = \begin{bmatrix} 0 & 0 \\ 0 & 0 \end{bmatrix} \tag{6}$$

and are the state matrix (**A**), the input matrix (**B**), the output matrix (**C**) and the direct-transmission matrix (**D**). Symbolically, $\{\mathbf{A},\mathbf{C}\} \in \mathscr{M}_{2\times 2}$ and $\{\mathbf{B},\mathbf{D}\} \in \mathscr{M}_{2\times 1}$. Regarding the assumption $\mathbf{x}(t) = \mathbf{y}(t)$, it should be noted that in a state-space model such as (5), the vector $\mathbf{x}(t)$ and the output vector $\mathbf{y}(t)$ are related, but not necessarily equivalent. In fact, the state vector $\mathbf{x}(t)$ represents the internal state variables of the system, which describe the current state of the system. The output vector $\mathbf{y}(t)$, on the other hand, represents the measurable or observable quantities of interest [25].

In many cases, the vector $\mathbf{y}(t)$ may be a subset of the vector $\mathbf{x}(t)$, which means that some state variables may correspond to measured outputs [25]. In this study, the state variables are measured variables of the CEA. Therefore, as can be seen, there is a direct relationship between $\mathbf{x}(t)$ and $\mathbf{y}(t)$.

Also, from (5) *hie* and R_o are defined as follows:

$$hib = \frac{V_T}{I_{E_Q}}, hie = \beta \cdot hib \tag{7}$$

$$R_o = R_C || R_L \tag{8}$$

From (7), V_T is the thermal voltage, which is 26 mV [17, 18]. From (6) the expression of k and R_i are defined as follows:

$$k = \frac{\beta \cdot R_i}{hie + \beta \cdot R_E} \tag{9}$$

$$R_i = R_B || (hie + \beta \cdot R_E) \tag{10}$$

Given the linear nature of the model in (5), further conversion of (5) to the Laplace domain (s) is performed. The s-domain converted model is defined as follows:

$$\begin{bmatrix} s + \frac{R_i}{L} & 0 \\ \frac{k}{L} & s + \frac{1}{R_o \cdot C} \end{bmatrix} \cdot \begin{bmatrix} I_i(s) \\ V_o(s) \end{bmatrix} = \begin{bmatrix} \frac{V_i(s)}{L} \\ 0 \end{bmatrix} \tag{11}$$

Taking (11) and assuming that $s = j\cdot\omega$, the CEA gain expression in the frequency domain is derived and defined as follows:

$$\mathbf{A_v}(j \cdot \omega) = -\frac{k}{L} \cdot \frac{j \cdot \omega + \frac{R_i}{L}}{j \cdot \omega + \frac{1}{R_o \cdot C}} \tag{12}$$

In order to verify the amplifying effect of this device, the Bode diagram of the gain $\mathbf{A_v}(j\cdot\omega)$ is plotted and shown in Figure 4. The parameters of this CEA given in Table 1 are used for this plot. It is important to note that the data presented in Table 1 were extracted from [24], and are part of a theoretical design.

Table 1. Common-emitter amplifier simulation parameters [24]

Parameters	Values
R_1	3 kΩ
R_2	15 kΩ
R_C	2 kΩ
R_E	500 Ω
R_L	1 kΩ
L	10 mH
C	100 pF
V_{cc}	24 V
V_γ	0.7 V

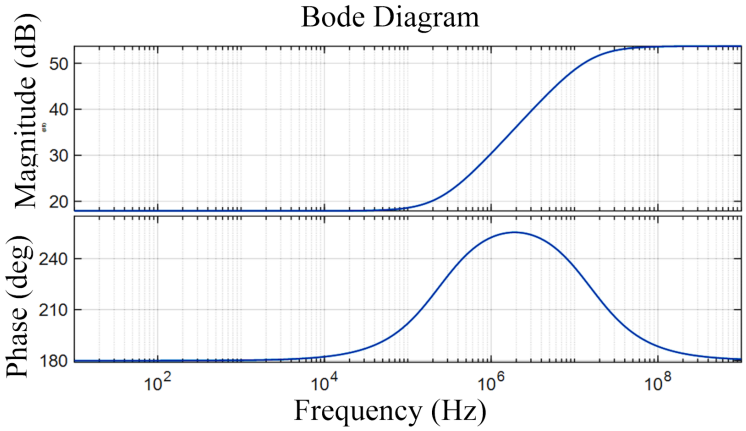

Figure 4. Bode diagram of $\mathbf{A_v}(j\cdot\omega)$. At low frequencies the $\mathbf{A_v}(j\cdot\omega) \approx 18$ dB and phase reach 180°. At high frequencies, the $\mathbf{A_v}(j\cdot\omega) \approx 54$ dB

From (12) and the information that can be taken from Figure 4, it can be seen that the CEA is indeed an inverter. On the other hand, at low frequencies the CEA has an approximately constant gain of 18 dB and then at high frequencies the gain is increased to 54 dB. It can also be seen that the phase of $\mathbf{A_v}(j\cdot\omega)$ remains constant at 180° (which justifies the inverter nature of the CEA) and after 10 kHz the phase increases until it reaches a maximum of 255° at 300 kHz. Then, as the frequency increases, the phase decreases until it returns to 180°.

4. Park and Clarke transformation analysis

The Clarke (α-β-0) and Park (d-q-0) transformations play a crucial role in the field of electricity and power electronics, and are widely recognized for their versatile applications [26, 27, 28, 29, 30]. These transformations are fundamental methods for converting three-phase quantities, such as voltages or currents, from the conventional a-b-c reference frame to the d-q-0 reference frame. In the a-b-c reference frame, each phase is represented as a sinusoidal function with a 120° phase shift, which is the natural coordinate system for three-phase systems. In contrast, the d-q-0 reference frame is a rotating coordinate system that is carefully aligned with either the magnetic flux of a machine or the voltage vector of an inverter. Within the d-q-0 reference frame, two orthogonal axes, known as the d-axis and the q-axis, correspond exactly to the direct and quadrature components of the three-phase magnitude. In addition, the d-q-0 reference frame includes a zero-sequence component that effectively represents the common-mode or neutral aspect of the three-phase magnitude [22].

These transformations, α-β-0 and d-q-0, are intrinsically linked by a rotation matrix. The α-β-0 transformation transforms a-b-c quantities into stationary α-β-0 quantities that are aligned with the stationary axes of the machine or

drive. Conversely, the d-q-0 transformation takes these stationary α-β-0 quantities and transforms them into dynamic d-q-0 quantities that are precisely aligned with the rotating axes of the machine or drive. The exact angle of rotation in d-q-0 depends on the angular position or speed of the machine or drive [22].

In addition, α-β-0 and d-q-0 offer a variety of advantages in the three-phase domain. They simplify the mathematical representation of these systems by reducing them to single- or two-phase models, which greatly reduces computational complexity. In addition, these transformations decouple the active and reactive power components, effectively splitting them into d and q components, allowing a deeper understanding and control of power distribution. In addition, they enable the implementation of vector control techniques in machines and inverters, providing direct control over critical parameters such as torque, flux, voltage, and current, ultimately improving system performance and efficiency [22].

In essence, the α-β-0 and d-q-0 transformations provide essential bridges between the conventional a-b-c and d-q-0 reference frames, making three-phase electrical systems more understandable and controllable. Their solid mathematical foundations and versatile applications are central to the fields of power electronics and electrical engineering.

4.1 *Derivation of the Clarke transformation matrix*

The α-β-0 transformation, a powerful tool in electrical engineering, functions as an essential bridge between vectors in the conventional a-b-c reference frame and the α-β-0 reference frame. Its primary strength lies in its remarkable ability to disentangle the components of an a-b-c-referenced vector by emphasizing the common element shared by all three vector components-in particular, it emphasizes the common-mode component, often referred to as the Z component [22, 31]. This transformation is supported by a number of features: it maintains power invariance, adheres to right-handed coordinate system conventions, and follows uniform scaling principles [22, 31]. The core of this transformation is represented by the power-invariant, right-handed, uniformly scaled Clarke transform matrix defined as follows

$$\mathbf{K_C}=\sqrt{\frac{2}{3}}\cdot\begin{bmatrix}1 & -\frac{1}{2} & -\frac{1}{2}\\ 0 & \frac{\sqrt{3}}{2} & -\frac{\sqrt{3}}{2}\\ \frac{1}{\sqrt{2}} & \frac{1}{\sqrt{2}} & \frac{1}{\sqrt{2}}\end{bmatrix} \tag{13}$$

To convert an abc-referenced system represented as a time-domain column vector ($\mathbf{m_{abc}}(t)$) into a corresponding time-domain column vector in the α-β-0 reference frame ($\mathbf{m_{\alpha\beta0}}(t)$), the a-b-c vector must undergo a pre-multiplication process with the transformation matrix $\mathbf{K_C}$, as shown in follows

$$\mathbf{m_{\alpha\beta0}}(t)=\mathbf{K_c}\cdot\mathbf{m_{abc}}(t) \tag{14}$$

On the other hand, to return to the a-b-c frame (i.e., $\mathbf{m_{\alpha\beta0}}$ (t)), both sides of (14) must be pre-multiplied by the inverse of $\mathbf{K_C}$, resulting in the following expression

$$\mathbf{m_{abc}}(t)=\mathbf{K_c}^{-1}\cdot\mathbf{m_{\alpha\beta0}}(t) \tag{15}$$

In essence, the α-β-0 transformation is a fundamental tool in electrical engineering that simplifies the manipulation of vectors between the a-b-c and α-β-0 reference frames while preserving important mathematical properties and conventions.

4.2 *Derivation of the Park transformation matrix*

The d-q-0 transformation plays a central role in the conversion of vectors originating in the α-β-0 reference frame to the d-q-0 reference frame, and has considerable utility in various applications [22, 31]. Its primary function is to facilitate a controlled realignment of a vector's reference frame, a process often referred to as "soft rotation," which occurs at a user-defined frequency. One of its critical features is the precise manipulation of a signal's frequency spectrum. This manipulation allows the user-specified frequency to appear as a dc frequency while simultaneously inverting the original dc

frequency to match the specified frequency. This transformation effectively recalibrates the frequency alignment, making it a fundamental tool in numerous engineering and control contexts [22, 31].

Mathematically, the d-q-0 transformation is expressed in its matrix representation, defined as follows

$$\mathbf{K_P} = \begin{bmatrix} \cos\theta(t) & \sin\theta(t) & 0 \\ -\sin\theta(t) & \cos\theta(t) & 0 \\ 0 & 0 & 1 \end{bmatrix} \tag{16}$$

Here, $\theta(t)$ represents the instantaneous angle corresponding to an arbitrary angular frequency ($\omega(t)$) [22, 31]. To convert a time-domain column vector in the α-β-0 reference frame, denoted $\mathbf{m_{\alpha\beta 0}}(t)$, into a new time-domain column vector in the d-q-0 reference frame, $\mathbf{m_{dq0}}(t)$, the following expression must be satisfied

$$\mathbf{m_{dq0}}(t) = \mathbf{K_P} \cdot \mathbf{m_{\alpha\beta 0}}(t) \tag{17}$$

Similarly, to return to the α-β-0 frame, the inverse transformation is required, given by

$$\mathbf{m_{\alpha\beta 0}}(t) = \mathbf{K_P}^{-1} \cdot \mathbf{m_{dq0}}(t) \tag{18}$$

Extending the previous information, it is possible to derive the transformation matrix from directly transforming a time-domain column vector from the a-b-c reference frame into a new time-domain column vector in the d-q-0 reference frame. This matrix is derived as $\mathbf{K_{CP}} = \mathbf{K_C} \cdot \mathbf{K_P}$, resulting in

$$\mathbf{K_{CP}} = \sqrt{\frac{2}{3}} \cdot \begin{bmatrix} \cos\theta(t) & \cos\left(\theta(t) - \frac{2\cdot\pi}{3}\right) & \cos\left(\theta(t) + \frac{2\cdot\pi}{3}\right) \\ -\sin\theta(t) & -\sin\left(\theta(t) - \frac{2\cdot\pi}{3}\right) & -\sin\left(\theta(t) + \frac{2\cdot\pi}{3}\right) \\ \frac{\sqrt{2}}{2} & \frac{\sqrt{2}}{2} & \frac{\sqrt{2}}{2} \end{bmatrix} \tag{19}$$

It should be noted that inverse transform of (19) is defined in (20). For the direct conversion of a time column vector referenced in abc ($\mathbf{m_{abc}}(t)$) into a time column vector in the d-q-0 frame ($\mathbf{m_{dq0}}(t)$), (21) is used. Conversely, for a return to the abc frame, (22) also is used.

In a geometric context, the d-q-0 transformation, much like the α-β-0 transformation, is rooted in

$$\mathbf{K_{CP}}^{-1} = \sqrt{\frac{2}{3}} \cdot \begin{bmatrix} \cos\theta(t) & -\sin\theta(t) & \frac{\sqrt{2}}{2} \\ \cos\left(\theta(t) - \frac{2\cdot\pi}{3}\right) & -\sin\left(\theta(t) - \frac{2\cdot\pi}{3}\right) & \frac{\sqrt{2}}{2} \\ \cos\left(\theta(t) + \frac{2\cdot\pi}{3}\right) & -\sin\left(\theta(t) + \frac{2\cdot\pi}{3}\right) & \frac{\sqrt{2}}{2} \end{bmatrix} \tag{20}$$

$$\mathbf{m_{dq0}}(t) = \mathbf{K_{CP}} \cdot \mathbf{m_{abc}}(t) \tag{21}$$

$$\mathbf{m_{abc}}(t) = \mathbf{K_{CP}}^{-1} \cdot \mathbf{m_{dq0}}(t) \tag{22}$$

the principles of dot products and vector projections [22, 31]. To illustrate this concept, consider an α-β reference frame and a dq reference frame displayed simultaneously (see Figure 5). The 0 coordinate is intentionally omitted in both reference frames for clarity. In this scenario, a vector is displayed in the α-β frame, $\mathbf{m_{\alpha\beta}}(t)$. Note that the dq frame is shifted by $\theta(t)$ degrees from the α-β reference frame.

The Cartesian representation of $\mathbf{m_{\alpha\beta}}(t)$ in terms of the α-β frame is defined as

$$\mathbf{m}_{\boldsymbol{\alpha\beta}}(t) = \mathbf{m}_{\boldsymbol{\alpha}}(t) \cdot \hat{\mathbf{u}}_{\boldsymbol{\alpha}} + \mathbf{m}_{\boldsymbol{\beta}}(t) \cdot \hat{\mathbf{u}}_{\boldsymbol{\beta}} \tag{23}$$

Here, $\hat{\mathbf{u}}_{\boldsymbol{\alpha}}$ and $\hat{\mathbf{u}}_{\boldsymbol{\beta}}$ denote the unit basis vectors corresponding to the α and β components of the α-β reference frame. The angle $\theta(t)$ represents the orientation between $\hat{\mathbf{u}}_{\boldsymbol{\alpha}}$ and $\hat{\mathbf{u}}_{\mathbf{d}}$ [22, 31]. Referring to Figure 5, the unitary vectors for the d and q components with respect to the α and β components can be defined as follows

$$\begin{cases} \hat{\mathbf{u}}_{\mathbf{d}} = \cos(\theta(t)) \cdot \hat{\mathbf{u}}_{\boldsymbol{\alpha}} + \sin(\theta(t)) \cdot \hat{\mathbf{u}}_{\boldsymbol{\beta}} \\ \hat{\mathbf{u}}_{\mathbf{q}} = -\sin(\theta(t)) \cdot \hat{\mathbf{u}}_{\boldsymbol{\alpha}} + \cos(\theta(t)) \cdot \hat{\mathbf{u}}_{\boldsymbol{\beta}} \end{cases} \tag{24}$$

The projection of the vector $\mathbf{m}_{\boldsymbol{\alpha\beta}}(t)$ onto the unit vectors of the d and q frames, i.e., $\hat{\mathbf{u}}_{\mathbf{d}}$ and $\hat{\mathbf{u}}_{\mathbf{q}}$, can be understood through the concept of the dot product where $\mathbf{m}_{\mathbf{d}}(t)$ represents the projection of $\mathbf{m}_{\boldsymbol{\alpha\beta}}(t)$ onto the $\hat{\mathbf{u}}_{\mathbf{d}}$ axis, and $\mathbf{m}_{\mathbf{q}}(t)$ represents the projection onto the $\hat{\mathbf{u}}_{\mathbf{q}}$ axis as can be seen as follows

$$\begin{cases} \mathbf{m}_{\mathbf{d}}(t) = \hat{\mathbf{u}}_{\mathbf{d}} \cdot \mathbf{m}_{\boldsymbol{\alpha\beta}}(t) = \\ = \cos(\theta(t)) \cdot \mathbf{m}_{\boldsymbol{\alpha}}(t) + \sin(\theta(t)) \cdot \mathbf{m}_{\boldsymbol{\beta}}(t) \\ \mathbf{m}_{\mathbf{q}}(t) = \hat{\mathbf{u}}_{\mathbf{q}} \cdot \mathbf{m}_{\boldsymbol{\alpha\beta}}(t) = \\ = -\sin(\theta(t)) \cdot \mathbf{m}_{\boldsymbol{\alpha}}(t) + \cos(\theta(t)) \cdot \mathbf{m}_{\boldsymbol{\beta}}(t) \end{cases} \tag{25}$$

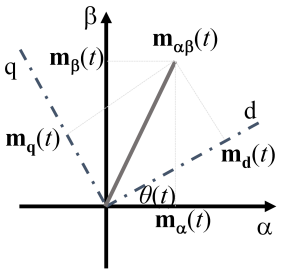

Figure 5. Geometric representation of an arbitrary vector $\mathbf{m}_{\boldsymbol{\alpha\beta}}(t)$ in reference frames αβ and dq. In addition, the vector components of the vector in its two reference frames are included

Together, these projected components, $\mathbf{m}_{\mathbf{d}}(t)$ and $\mathbf{m}_{\mathbf{q}}(t)$, constitute the new vector, $\mathbf{m}_{\mathbf{dq}}(t)$, within the d-q reference frame [22, 31]. It is important to note that the positive angle $\theta(t)$ corresponds to a counter-clockwise rotation of the vector as it transitions to the new d-q reference frame. This implies that the angle of the vector relative to the new reference frame is smaller than its angle within the old reference frame (i.e., the α-β reference frame). This difference arises from the fact that it is the reference frame itself that has undergone a forward rotation, not the vector. In essence, a forward rotation of the reference frame is equivalent to a negative rotation of the vector. In scenarios where the original reference frame experiences a forward rotation, such as in three-phase electrical systems, the resulting d-q vector ($\mathbf{m}_{\mathbf{dq}}(t)$) essentially maintains its position without further rotation [22, 31]. In this analysis, two-component column vectors, ($\mathbf{m}_{\boldsymbol{\alpha}}(t)$, $\mathbf{m}_{\boldsymbol{\beta}}(t)$) and ($\mathbf{m}_{\mathbf{d}}(t)$, $\mathbf{m}_{\mathbf{q}}(t)$), for the α-β and d-q reference frames, respectively. Thus, a 2 × 2 matrix containing these column vectors is defined as

$$\mathbf{K}_{\mathbf{P}} = \begin{bmatrix} \cos\theta(t) & \sin\theta(t) \\ -\sin\theta(t) & \cos\theta(t) \end{bmatrix} \tag{26}$$

This matrix establishes the relationship expressed as $\mathbf{m}_{\mathbf{dq}}(t) = \mathbf{K}_{\mathbf{P}} \cdot \mathbf{m}_{\boldsymbol{\alpha\beta}}(t)$.

In cases where a single vector quantity consists of a single component, such as $\mathbf{m_a}(t)$, a direct application of the transformation defined in (21) may not be straightforward. However, the transformation associated with (26) can be used, as explained after in [32]. Like the core idea is to apply the Clarke transformation to the vector $\mathbf{m_a}(t)$, but in a simplified way. In particular, the transformation is defined as follows

$$\begin{cases} \mathbf{m_\alpha}(t) = \mathbf{m_a}(t) \\ \mathbf{m_\beta}(t) = \mathbf{m_a}\left(t - \frac{\pi}{2}\right) \end{cases} \tag{27}$$

where $\mathbf{m_\alpha}(t)$ and $\mathbf{m_\beta}(t)$ denote the components of $\mathbf{m_a}(t)$ in the α-β frame. This transformation retains the original component as $\mathbf{m_\alpha}(t)$, while the β component, $\mathbf{m_\beta}(t)$, corresponds to the original vector shifted by 90 degrees. Consequently, the vector $\mathbf{m_{\alpha\beta}}(t) = [\mathbf{m_\alpha}(t), \mathbf{m_\beta}(t)]^{\mathrm{T}}$ can be converted into $\mathbf{m_{dq}}(t)$ by applying (26) [22, 31].

5. Modeling of the common-emitter amplifier in d-q coordinates

A review of the model in (5) indicates that the d-q conversion is not directly applicable, given that (5) represents a single-phase system. However, as indicated in the previous section, by applying (27) to each of the single-phase variables in (5), a suitable model can be obtained for the application of (26). Consequently, each of the variables in (5) can be described as follows:

$$\begin{cases} i_{\mathrm{i}_\alpha}(t) = i_{\mathrm{i}}(t) \\ i_{\mathrm{i}_\beta}(t) = i_{\mathrm{i}}(t - 90^\circ) \end{cases} \begin{cases} v_{\mathrm{o}_\beta}(t) = v_{\mathrm{o}}(t - 90^\circ) \\ v_{\mathrm{i}_\beta}(t) = v_{\mathrm{i}}(t - 90^\circ) \end{cases} \begin{cases} v_{\mathrm{i}_\alpha}(t) = v_{\mathrm{i}}(t) \\ v_{\mathrm{i}_\beta}(t) = v_{\mathrm{i}}(t - 90^\circ) \end{cases} \tag{28}$$

Replacing the variables defined in (28) in (5), the state-space model in α-β coordinates is derived and given as

$$\begin{cases} \dot{\mathbf{x}}_{\alpha\beta}(t) = \mathbf{A}_{\alpha\beta} \cdot \mathbf{x}_{\alpha\beta}(t) + \mathbf{B}_{\alpha\beta} \cdot \mathbf{u}_{\alpha\beta}(t) \\ \mathbf{y}_{\alpha\beta}(t) = \mathbf{C}_{\alpha\beta} \cdot \mathbf{x}_{\alpha\beta}(t) + \mathbf{D}_{\alpha\beta} \cdot \mathbf{u}_{\alpha\beta}(t) \end{cases} \tag{29}$$

The matrices of the model in (29) are defined as follows:

$$\mathbf{A}_{\alpha\beta} = \begin{bmatrix} -\frac{R_\mathrm{i}}{L} & 0 & 0 & 0 \\ 0 & -\frac{R_\mathrm{i}}{L} & 0 & 0 \\ -\frac{k}{C} & 0 & -\frac{1}{R_\mathrm{o} \cdot C} & 0 \\ 0 & -\frac{k}{C} & 0 & -\frac{1}{R_\mathrm{o} \cdot C} \end{bmatrix}, \mathbf{B}_{\alpha\beta} = \begin{bmatrix} \frac{1}{L} & 0 \\ 0 & \frac{1}{L} \\ 0 & 0 \\ 0 & 0 \end{bmatrix}, \mathbf{C}_{\alpha\beta} = \begin{bmatrix} 1 & 0 & 0 & 0 \\ 0 & 1 & 0 & 0 \\ 0 & 0 & 1 & 0 \\ 0 & 0 & 0 & 1 \end{bmatrix}, \mathbf{D}_{\alpha\beta} = \begin{bmatrix} 0 & 0 & 0 & 0 \\ 0 & 0 & 0 & 0 \\ 0 & 0 & 0 & 0 \\ 0 & 0 & 0 & 0 \end{bmatrix} \tag{30}$$

On the other hand, the vectors are defined as $\mathbf{x_{\alpha\beta}}(t) = [i_{\mathrm{i}\alpha}(t), i_{\mathrm{i}\beta}(t), v_{\mathrm{o}\alpha}(t), v_{\mathrm{o}\beta}(t)]^{\mathrm{T}}$, $\mathbf{u_{\alpha\beta}}(t) = [v_{\mathrm{i}\alpha}(t), v_{\mathrm{i}\beta}(t)]^{\mathrm{T}}$, and $\mathbf{y_{\alpha\beta}}(t) = \mathbf{x_{\alpha\beta}}(t)$. Symbolically, $\mathbf{u_{\alpha\beta}}(t) \in \{\mathbb{R}^2\}$ and $\{\mathbf{x_{\alpha\beta}}(t), \mathbf{y_{\alpha\beta}}(t)\} \in \{\mathbb{R}^4\}$ and $\{\mathbf{A}_{\alpha\beta}, \mathbf{C}_{\alpha\beta}\} \in \mathscr{M}_{4\times4}$ and $\{\mathbf{B}_{\alpha\beta}, \mathbf{D}_{\alpha\beta}\} \in \mathscr{M}_{4\times2}$.

Park's transformation is directly applied to the given model in α-β coordinates derived in (29) [22]. The d-q coordinate model of the system is defined as follows:

$$\begin{cases} \dot{\mathbf{x}}_{\mathbf{dq}}(t) = \mathbf{A_{dq}} \cdot \mathbf{x_{dq}}(t) + \mathbf{B_{dq}} \cdot \mathbf{u_{dq}}(t) \\ \mathbf{y_{dq}}(t) = \mathbf{C_{dq}} \cdot \mathbf{x_{dq}}(t) + \mathbf{D_{dq}} \cdot \mathbf{u_{dq}}(t) \end{cases} \tag{31}$$

Note that, the d-q transformation operates properly when the unconverted variables be pure sinusoidal [22].

Finally, the matrices of the model are defined in (32), where k is defined in (9). The vectors are defined as $\mathbf{x_{dq}}(t) = [i_{\mathrm{id}}(t), i_{\mathrm{iq}}(t), v_{\mathrm{od}}(t), v_{\mathrm{oq}}(t)]^{\mathrm{T}}$, $\mathbf{u_{dq}}(t) = [v_{\mathrm{id}}(t), v_{\mathrm{iq}}(t)]^{\mathrm{T}}$, and $\mathbf{y_{dq}}(t) = \mathbf{x_{dq}}(t)$. Symbolically, $\mathbf{u_{dq}}(t) \in \{\mathbb{R}^2\}$, $\{\mathbf{x_{dq}}(t), \mathbf{y_{dq}}(t)\}$

$\in\{\mathbb{R}^4\}$, $\{\mathbf{A}_{dq}, \mathbf{C}_{dq}\} \in \mathscr{M}_{4\times4}$, and $\{\mathbf{B}_{dq}, \mathbf{D}_{dq}\} \in \mathscr{M}_{4\times2}$. Also, from the matrices, $\omega = 2\cdot\pi\cdot f$, where f is the input-voltage frequency.

The linear model in d-q coordinates of the CEA defined in (16) is illustrated diagrammatically in Figure 6. The CEA model in d-q coordinates is configured by two decoupled networks associated with the d and q channels.

It can also be seen that each of the channels is configured by a voltage circuit and a current circuit. The voltage circuits contain current-controlled voltage sources and the current circuits contain current- and voltage-controlled current sources.

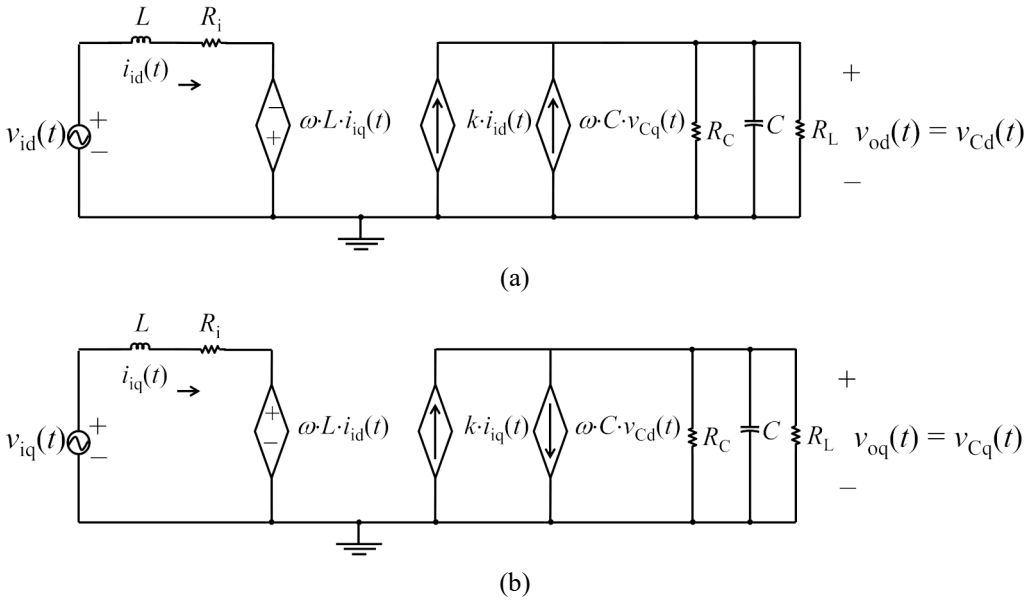

Figure 6. d-q model of the CEA. (**a**) d-channel. (**b**) q-channel

$$\mathbf{A}_{dq}=\begin{bmatrix} -\frac{R_i}{L} & \omega & 0 & 0 \\ -\omega & -\frac{R_i}{L} & 0 & \omega \\ -\frac{k}{C} & 0 & -\frac{1}{R_o\cdot C} & 0 \\ 0 & -\frac{k}{C} & -\omega & -\frac{1}{R_o\cdot C} \end{bmatrix}, \mathbf{B}_{dq}=\begin{bmatrix} \frac{1}{L} & 0 \\ 0 & \frac{1}{L} \\ 0 & 0 \\ 0 & 0 \end{bmatrix}, \mathbf{C}_{dq}=\begin{bmatrix} 1 & 0 & 0 & 0 \\ 0 & 1 & 0 & 0 \\ 0 & 0 & 1 & 0 \\ 0 & 0 & 0 & 1 \end{bmatrix}, \mathbf{D}_{dq}=\begin{bmatrix} 0 & 0 & 0 & 0 \\ 0 & 0 & 0 & 0 \\ 0 & 0 & 0 & 0 \\ 0 & 0 & 0 & 0 \end{bmatrix} \tag{32}$$

6. Dynamic equation solution

In order to obtain a deep understanding of the dynamics of the system state variables in both electric and d-q coordinates, it is necessary to obtain the expressions representing the dynamics of these variables, i.e., in the electric domain ($i_i(t)$ and $v_o(t)$) and in the d-q domain ($i_{id}(t)$, $i_{iq}(t)$, $v_{od}(t)$, and $v_{oq}(t)$). Therefore, it is necessary to solve the state equations presented in (5) for the electric case and in (31) for the d-q case. The solutions discussed above are developed below.

6.1 *Solution of the state equations in electrical coordinates*

From (5), the dynamic equations of the system in electric coordinates are given by:

$$\begin{cases} \frac{di_i(t)}{dt} = -\frac{R_i}{L}\cdot i_i(t) + \frac{1}{L}\cdot v_i(t) \\ \frac{dv_o(t)}{dt} = -\frac{k}{C}\cdot i_i(t) - \frac{1}{R_o\cdot C}\cdot v_o(t) \end{cases} \tag{33}$$

Considering that both differential equations shown in (33) are of first-order linear type, they can be solved by using integration factors [33]. For the case of the differential equation relating $i_i(t)$, assuming that $v_i(t) = V_i \cdot \sin(\omega \cdot t)$, where V_i and ω are the peak-to-peak voltage and angular frequency of $v_i(t)$, respectively, and applying the integration factor (IF) defined as $IF = e^{\frac{t}{\tau_L}}$, in both sides of the differential equation relating $i_i(t)$, the expression of $i_i(t)$ is obtained and defined as

$$i_i(t) = I_i \cdot \sin(\omega \cdot t - \phi) + I'_{i_o} \cdot e^{-\frac{t}{\tau_L}} \tag{34}$$

where I_i, I'_{io}, τ_L, and φ are the steady state magnitude, the transient magnitude, the inductive time constant, and the phase shift angle, respectively. The definitions of each of these constants are given by

$$\begin{cases} I_i = \frac{V_i}{\sqrt{R_i^2 + \omega^2 \cdot L^2}} \\ I'_{i_o} = I_{i_o} + \omega \cdot L \cdot \frac{V_i}{R_i^2 + \omega^2 \cdot L^2} \\ \tau_L = \frac{L}{R_i} \\ \phi = \tan^{-1}\left(\frac{\omega \cdot L}{R_i}\right) \end{cases} \tag{35}$$

Also, I_{io} is the initial system current. As is trivial, $i_i(t)$ has two components, one in the transient regime and the other in the steady state. In addition, the magnitude of I_i depends strongly on the real component of the inductive input impedance formed by R_i and the inductive reactance $\mathbf{X_L}(j \cdot \omega) = j \cdot \omega \cdot L$. The magnitude I'_{io} also depends on the initial current and a current source determined by $\mathbf{X_L}(j \cdot \omega)$ and controlled by the current I_i. Finally, τ_L corresponds to the time constant generated by the input circuit formed by R_i and $\mathbf{X_L}(j \cdot \omega)$. To solve the differential equation for the variable $v_o(t)$, the $IF = e^{\frac{t}{\tau_C}}$ is applied, also in both sides of the differential equation relating $v_o(t)$, obtaining the expression of $v_o(t)$ defined by:

$$v_o(t) = -V_o \cdot \cos(\omega \cdot t - \phi + \theta) - V_{o_1} \cdot e^{-\frac{t}{\tau_L}} + V'_{o_o} \cdot e^{-\frac{t}{\tau_C}} \tag{36}$$

The expressions V_o, V_{oo1}, V'_{oo}, τ_C, and θ are given by:

$$\begin{cases} V_o = -\frac{k \cdot I_i \cdot \tau_C}{C \cdot \sqrt{1 + \omega^2 \cdot \tau_C^2}} \\ V_{o_1} = \frac{k \cdot I'_{i_o} \cdot \tau_L \cdot \tau_C}{C \cdot (\tau_L - \tau_C)} \\ V'_{o_o} = V_{o_o} - \frac{k \cdot \tau_C \cdot (\sin\phi + \omega \cdot \tau_C \cdot \cos\phi)}{C \cdot (1 + \omega^2 \cdot \tau_C^2)} + V_{o_1} \\ \tau_C = R_o \cdot C \\ \theta = \tan^{-1}\left(\frac{1}{\omega \cdot \tau_C}\right) \end{cases} \tag{37}$$

From reference (36), it can be confirmed that the behavior of $v_o(t)$ dynamics is straightforward, as it consists of two components: a transient component and a steady-state component. Additionally, it is observable that the transient stage is comprised of two subparts. During the steady state stage, it is evident that the output network consisting of R_o and C affects the magnitude of V_o, as stated in (37).

Additionally, the magnitude of the steady state current $i_i(t)$ also impacts V_o. The R_i-L and R_o-C networks influence V_{oo1}'s magnitude during the transient period, as per (37), due to the greater impact of the inductive and capacitive time constants. It is worth noting that τ_L and τ_C affect the transient components related to the magnitudes of V_{oo1} and V'_{oo}, respectively. Finally, it can be analyzed that

V'_{oo}'s magnitude depends on the phase difference angle φ, and θ has a direct dependence on the R_o-C network's dynamics.

6.2 *Solution of the state equations in d-q coordinates*

As in Subsection 5.1, the system's dynamic equations in d-q coordinates are obtained from (16) and presented in (38). Note that by applying the d-q transformation described in Section 4 to the voltage source $v_{\mathrm{i}}(t)$, the source channels d and q are obtained and defined as $v_{\mathrm{id}}(t) = 0$ and $v_{\mathrm{iq}}(t) = V_{\mathrm{i}}$.

As in the previous case (Subsection 5.1), the dynamic equations of the system in d-q coordinates are obtained from (16) and presented as follows:

$$\begin{cases} \frac{\mathrm{d}i_{\mathrm{i_d}}(t)}{\mathrm{d}t} = -\frac{R_{\mathrm{i}}}{L}\cdot i_{\mathrm{i_d}}(t) + \omega \cdot i_{\mathrm{i_q}}(t) \\ \frac{\mathrm{d}i_{\mathrm{i_q}}(t)}{\mathrm{d}t} = -\omega \cdot i_{\mathrm{i_d}}(t) - \frac{R_{\mathrm{i}}}{L}\cdot i_{\mathrm{i_q}}(t) + \omega \cdot v_{\mathrm{o_q}}(t) + \frac{1}{L}\cdot V_{\mathrm{i}} \\ \frac{\mathrm{d}v_{\mathrm{o_d}}(t)}{\mathrm{d}t} = -\frac{k}{C}\cdot i_{\mathrm{i_d}}(t) - \frac{1}{R_{\mathrm{o}}\cdot C}\cdot v_{\mathrm{o_d}}(t) \\ \frac{\mathrm{d}v_{\mathrm{o_q}}(t)}{\mathrm{d}t} = -\frac{k}{C}\cdot i_{\mathrm{i_q}}(t) - \omega \cdot v_{\mathrm{o_d}}(t) - \frac{1}{R_{\mathrm{o}}\cdot C}\cdot v_{\mathrm{o_q}}(t) \end{cases} \tag{38}$$

Note that by applying the d-q transformation described in Section 4 to the voltage source $v_{\mathrm{i}}(t)$, the source channels d and q are obtained and defined as $v_{\mathrm{id}}(t) = 0$ and $v_{\mathrm{iq}}(t) = V_{\mathrm{i}}$. From (38) it can be seen that the differential equations related to the CEA in d-q coordinates are of the linear type with constant coefficients [34]. To solve this system, different methods are used. First, the differential operator $D = \mathrm{d}/\mathrm{d}t$ is applied to the system in (38), which transforms the equations in (38) into a system of non-differential linear equations. Thus, by applying D to (38), the new version of the latter is described as follows:

$$\begin{bmatrix} D+\frac{R_{\mathrm{i}}}{L} & -\omega & 0 & 0 \\ \omega & D+\frac{R_{\mathrm{i}}}{L} & 0 & -\omega \\ \frac{k}{C} & 0 & D+\frac{1}{R_{\mathrm{o}}\cdot C} & 0 \\ 0 & \frac{k}{C} & \omega & D+\frac{1}{R_{\mathrm{o}}\cdot C} \end{bmatrix} \cdot \begin{bmatrix} i_{\mathrm{i_d}}(t) \\ i_{\mathrm{i_q}}(t) \\ v_{\mathrm{o_d}}(t) \\ v_{\mathrm{o_q}}(t) \end{bmatrix} = \begin{bmatrix} 0 \\ \frac{V_{\mathrm{i}}}{L} \\ 0 \\ 0 \end{bmatrix} \tag{39}$$

To obtain the solution of this system, the complementary and particular components of each of the state variables of the system in (39) are derived. The components of the state variables are derived as follows. Note that to obtain these components, the constant column vector on the right side of (39) must be forced to zero [34]. By doing this, one can see that the complementary component of each of the variables is the same. The derivation of these components is described in detail below.

6.2.1 *Derivation of the complementary component of the system's state variables in d-q coordinates*

In order to facilitate the derivation of the complementary components of the system in (39), an analogy of (39) is performed and the following matrix-equation system is obtained:

$$\mathbf{A}\cdot\mathbf{c} = \mathbf{0} \tag{40}$$

By comparing (39) and (40), one can easily define the **A**, the vector **c**. In this case, **0** is a null vector. Specifically, the vector **c** corresponds to the complementary components of the state variables being studied. Thus, $\mathbf{c} = [i^{\mathrm{c}}{}_{\mathrm{id}}(t), i^{\mathrm{c}}{}_{\mathrm{iq}}(t), v^{\mathrm{c}}{}_{\mathrm{od}}(t), v^{\mathrm{c}}{}_{\mathrm{oq}}(t)]^{\mathrm{T}}$. Symbolically, $\mathbf{A} \in \mathscr{M}_{4\times4}$, $\mathbf{0} \in \mathscr{M}_{4\times1}$, and $\mathbf{c} \in \{\mathbb{R}^4\}$. Within the framework of the solution method for this type of equations, the characteristic equation of the system is obtained, which consists in calculating the differential variable D, corresponding to the characteristic values, by solving the equation $\det(\mathbf{A}) = 0$ [34]. As a result, the expression in (40) can be defined in the following canonical form:

$$(D+D_1)(D+D_2)(D+D_3)(D+D_4)n = 0 \tag{41}$$

where $n(t) \in \{i^{c}_{id}(t), i^{c}_{iq}(t), v^{c}_{od}(t), v^{c}_{oq}(t)\}$. Due to the complexity of the solutions of D_i ($i \in \{1, 2, 3, 4\}$), they are not shown in explicitly way in this article. However, it can be verified that D_i values are as follows: $D_1 = -\alpha_1 + j\cdot\beta_1$, $D_2 = -\alpha_1 - j\cdot\beta_1$, $D_3 = -\alpha_2 + j\cdot\beta_2$, and $D_4 = -\alpha_2 - j\cdot\beta_2$. From this analysis, it is evident that the complementary components provide complex conjugate and stable variables ($\mathrm{Re}\{D_i\} < 0$). Equation (41) is elementary [33, 34] with a solution described as:

$$n(t) = e^{-\alpha_1 \cdot t} \cdot \left(C_1 \cdot e^{j\cdot\beta_1 \cdot t} + C_2 \cdot e^{-j\cdot\beta_1 \cdot t}\right) + e^{-\alpha_2 \cdot t} \cdot \left(C_3 \cdot e^{j\cdot\beta_2 \cdot t} + C_4 \cdot e^{-j\cdot\beta_2 \cdot t}\right) \tag{42}$$

This expression exhibits transient dynamics, as per the theory of solving differential equations.

6.2.2 *Derivation of the particular component of the system's state variables in d-q coordinates*

As previously stated, the system outlined in (37) is a linear differential equation system with constant coefficients. Accordingly, a practical technique for acquiring the particular components of the state variables involved in (37) is to solve each of the equations outlined in (38) as a first-order linear differential equation [34]. Therefore, in the case of the particular component of $i_{id}(t)$, i.e., $i^{p}_{id}(t)$, it can be defined as follows:

$$i^{p}_{id}(t) = \frac{1}{D+\alpha_1 - j\cdot\beta_1} \cdot \frac{1}{D+\alpha_1 + j\cdot\beta_1} \cdot \frac{1}{D+\alpha_2 - j\cdot\beta_2} \cdot \frac{1}{D+\alpha_2 + j\cdot\beta_2} \cdot L \cdot \omega \cdot V_i \tag{43}$$

Then, using the following change of variable, the first differential equation to be solved is given by:

$$u_1(t) = \frac{1}{D+\alpha_2 + j\cdot\beta_2} \cdot L \cdot \omega \cdot V_i \Rightarrow \frac{du_1(t)}{dt} + (\alpha_2 + j\cdot\beta_2) \cdot u_1(t) = L \cdot \omega \cdot V_i \tag{44}$$

In addition, the differential equation in (44) is trivially solved using the $IF = e^{(\alpha_2 + j\cdot\beta_2)\cdot t}$ and giving as the result:

$$u_1(t) = \frac{L \cdot \omega \cdot V_i}{\alpha_2 + j\cdot\beta_2} \tag{45}$$

Applying the following change of variable, the second differential equation to be solved is obtained as:

$$u_2(t) = \frac{1}{D+\alpha_2 - j\cdot\beta_2} \cdot u_1(t) \Rightarrow \frac{du_2(t)}{dt} + (\alpha_2 - j\cdot\beta_2) \cdot u_2(t) = \frac{L \cdot \omega \cdot V_i}{\alpha_2 + j\cdot\beta_2} \tag{46}$$

Applying the $IF = e^{(\alpha_2 - j\cdot\beta_2)\cdot t}$, gives the solution shown as follows:

$$u_2(t) = \frac{L \cdot \omega \cdot V_i}{{\alpha_2}^2 + {\beta_2}^2} \tag{47}$$

Applying the third change of variable

$$u_3(t) = \frac{1}{D+\alpha_1 + j\cdot\beta_1} \cdot u_2(t) \Rightarrow \frac{du_3(t)}{dt} + (\alpha_1 + j\cdot\beta_1) \cdot u_2(t) = \frac{L \cdot \omega \cdot V_i}{{\alpha_2}^2 + {\beta_2}^2} \tag{48}$$

the third differential equation to be solved is obtained by using $IF = e^{(\alpha_1 + j\cdot\beta_1)\cdot t}$, giving the variable defined as follows:

$$u_3(t) = \frac{L \cdot \omega \cdot V_i}{\left({\alpha_2}^2 + {\beta_2}^2\right) \cdot (\alpha_1 + j\cdot\beta_1)} \tag{49}$$

Finally, the particular component $i^{p}_{id}(t)$ is obtained by solving the following differential equation:

$$\begin{aligned} i^{\mathrm{p}}{}_{\mathrm{i_d}}(t) &= \frac{1}{D+\alpha_1-\mathrm{j}\cdot\beta_1}\cdot u_3(t) \\ \Rightarrow \frac{\mathrm{d}i^{\mathrm{p}}{}_{\mathrm{i_d}}(t)}{\mathrm{d}t} &+ (\alpha_1-\mathrm{j}\cdot\beta_1)\cdot u_3(t) = \frac{L\cdot\omega\cdot V_{\mathrm{i}}}{\left(\alpha_2{}^2+\beta_2{}^2\right)\cdot(\alpha_1+\mathrm{j}\cdot\beta_1)} \end{aligned} \tag{50}$$

and applying the $IF = \mathrm{e}^{(\alpha_1\,-\,\mathrm{j}\cdot\beta_1)\cdot t}$, the particular component $i^{\mathrm{p}}{}_{\mathrm{id}}(t)$ is obtained and defined as:

$$i^{\mathrm{p}}{}_{\mathrm{i_d}}(t) = \frac{L\cdot\omega\cdot V_{\mathrm{i}}}{\left(\alpha_1{}^2+\beta_1{}^2\right)\cdot\left(\alpha_2{}^2+\beta_2{}^2\right)} \approx I^{\mathrm{p}}{}_{\mathrm{i_d}} \tag{51}$$

which corresponds to a constant value. Proceeding in the same way as described above, the particular components $I^{\mathrm{p}}{}_{\mathrm{iq}}$, $V^{\mathrm{p}}{}_{\mathrm{od}}$, and $V^{\mathrm{p}}{}_{\mathrm{oq}}$ are obtained as follows:

$$\begin{cases} I^{\mathrm{p}}{}_{\mathrm{i_q}} \approx -\frac{R_{\mathrm{i}}\cdot V_{\mathrm{i}}}{\left(\alpha_1{}^2+\beta_1{}^2\right)\cdot\left(\alpha_2{}^2+\beta_2{}^2\right)} \\ V^{\mathrm{p}}{}_{\mathrm{o_d}} \approx -\frac{L\cdot k\cdot\omega\cdot R_{\mathrm{o}}\cdot V_{\mathrm{i}}}{\left(\alpha_1{}^2+\beta_1{}^2\right)\cdot\left(\alpha_2{}^2+\beta_2{}^2\right)} \\ V^{\mathrm{p}}{}_{\mathrm{o_q}} \approx \frac{k\cdot R_{\mathrm{o}}\cdot R_{\mathrm{i}}\cdot V_{\mathrm{i}}}{\left(\alpha_1{}^2+\beta_1{}^2\right)\cdot\left(\alpha_2{}^2+\beta_2{}^2\right)} \end{cases} \tag{52}$$

Having the complementary (41) and particular (51), (52) components of each state variable of CEA in d-q coordinates, the complete solution of these variables is defined as the sum of their components as

$$\begin{cases} i_{\mathrm{i_d}}(t) = i^{\mathrm{c}}{}_{\mathrm{i_d}}(t) + I^{\mathrm{p}}{}_{\mathrm{i_q}} \\ \Longrightarrow i_{\mathrm{i_d}}(t) = \mathrm{e}^{-\alpha_1\cdot t}\cdot\left(C_1\cdot\mathrm{e}^{\mathrm{j}\cdot\beta_1\cdot t}+C_2\cdot\mathrm{e}^{-\mathrm{j}\cdot\beta_1\cdot t}\right)+\mathrm{e}^{-\alpha_2\cdot t}\cdot\left(C_3\cdot\mathrm{e}^{\mathrm{j}\cdot\beta_2\cdot t}+C_4\cdot\mathrm{e}^{-\mathrm{j}\cdot\beta_2\cdot t}\right)+ \\ \quad +\frac{L\cdot\omega\cdot V_{\mathrm{i}}}{\left(\alpha_1{}^2+\beta_1{}^2\right)\cdot\left(\alpha_2{}^2+\beta_2{}^2\right)} \\ i_{\mathrm{i_q}}(t) = i^{\mathrm{c}}{}_{\mathrm{i_q}}(t) + I^{\mathrm{p}}{}_{\mathrm{i_q}} \\ \Longrightarrow i_{\mathrm{i_q}}(t) = \mathrm{e}^{-\alpha_1\cdot t}\cdot\left(C_1\cdot\mathrm{e}^{\mathrm{j}\cdot\beta_1\cdot t}+C_2\cdot\mathrm{e}^{-\mathrm{j}\cdot\beta_1\cdot t}\right)+\mathrm{e}^{-\alpha_2\cdot t}\cdot\left(C_3\cdot\mathrm{e}^{\mathrm{j}\cdot\beta_2\cdot t}+C_4\cdot\mathrm{e}^{-\mathrm{j}\cdot\beta_2\cdot t}\right)- \\ \quad -\frac{L\cdot k\cdot\omega\cdot R_{\mathrm{o}}\cdot V_{\mathrm{i}}}{\left(\alpha_1{}^2+\beta_1{}^2\right)\cdot\left(\alpha_2{}^2+\beta_2{}^2\right)} \\ v_{\mathrm{o_d}}(t) = v^{\mathrm{c}}{}_{\mathrm{o_d}}(t) + V^{\mathrm{p}}{}_{\mathrm{o_d}} \\ \Longrightarrow v_{\mathrm{o_d}}(t) = \mathrm{e}^{-\alpha_1\cdot t}\cdot\left(C_1\cdot\mathrm{e}^{\mathrm{j}\cdot\beta_1\cdot t}+C_2\cdot\mathrm{e}^{-\mathrm{j}\cdot\beta_1\cdot t}\right)+\mathrm{e}^{-\alpha_2\cdot t}\cdot\left(C_3\cdot\mathrm{e}^{\mathrm{j}\cdot\beta_2\cdot t}+C_4\cdot\mathrm{e}^{-\mathrm{j}\cdot\beta_2\cdot t}\right)+ \\ \quad +\frac{L\cdot k\cdot\omega\cdot R_{\mathrm{o}}\cdot V_{\mathrm{i}}}{\left(\alpha_1{}^2+\beta_1{}^2\right)\cdot\left(\alpha_2{}^2+\beta_2{}^2\right)} \\ v_{\mathrm{o_q}}(t) = v^{\mathrm{c}}{}_{\mathrm{o_q}}(t) + V^{\mathrm{p}}{}_{\mathrm{o_q}} \\ \Longrightarrow v_{\mathrm{o_q}}(t) = \mathrm{e}^{-\alpha_1\cdot t}\cdot\left(C_1\cdot\mathrm{e}^{\mathrm{j}\cdot\beta_1\cdot t}+C_2\cdot\mathrm{e}^{-\mathrm{j}\cdot\beta_1\cdot t}\right)+\mathrm{e}^{-\alpha_2\cdot t}\cdot\left(C_3\cdot\mathrm{e}^{\mathrm{j}\cdot\beta_2\cdot t}+C_4\cdot\mathrm{e}^{-\mathrm{j}\cdot\beta_2\cdot t}\right)- \\ \quad -\frac{k\cdot R_{\mathrm{o}}\cdot R_{\mathrm{i}}\cdot V_{\mathrm{i}}}{\left(\alpha_1{}^2+\beta_1{}^2\right)\cdot\left(\alpha_2{}^2+\beta_2{}^2\right)} \end{cases} \tag{53}$$

It can be observed from the expressions presented in (53) that the dynamics of the system's state variables in d-q coordinates comprise of two stages-one transient and one in a steady-state regime. Moreover, it can be verified that the steady-state component is of the constant type, as expected in the dynamics converted to d-q coordinates.

7. Simulation results

The models defined by (5) and (10) are simulated using MATLAB-Simulink. The CEA is supplied with a sinusoidal voltage with an amplitude of 5 mV peak-to-peak and a frequency of 5 kHz. The parameters of the CEA are outlined in Table 1.

The simulation results under transient conditions related to (5) and (16) are shown in Figures 7 and 8, respectively. Additionally, Figure 9 shows the simulation results, under transient conditions, after the transformation of the system into d-q variables as defined in (5).

The dynamics of the current $i_i(t)$ are shown in Figure 6a, and the output voltage $v_o(t)$ is shown in Figure 6b. It is evident from Figure 6a that the CEA dynamics are sinusoidal, as $i_i(t)$ follows a sinusoidal pattern. Figure 6b demonstrates the gain and phase shift introduced by the CEA in the output voltage $v_o(t)$.

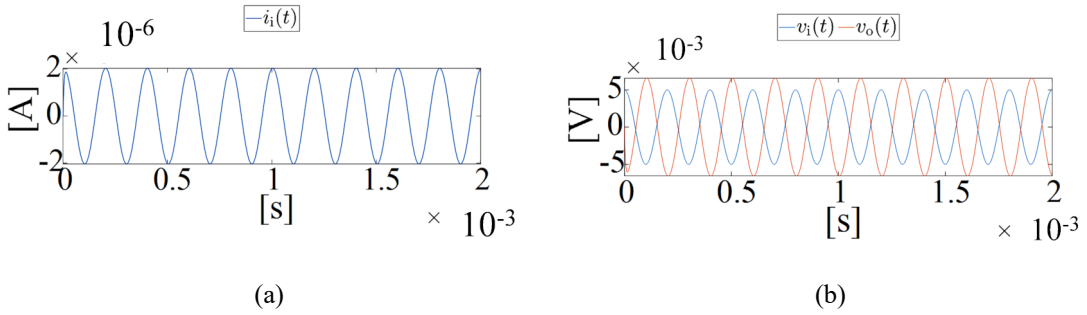

(a) (b)

Figure 7. Simulation results, under transients, regarding the dynamic variables from (5). (**a**) Input current $i_i(t)$. (**b**) Input and output voltages $v_i(t)$ and $v_o(t)$

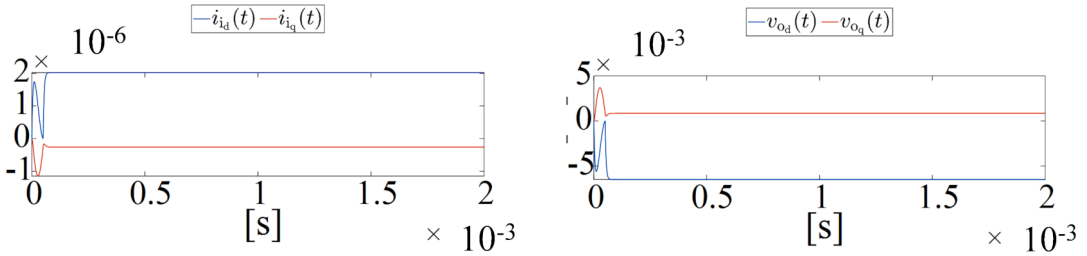

(a) (b)

Figure 8. Simulation results, under transients, regarding the dynamic variables from (16). (**a**) d- and q-channel of $i_i(t)$. (**b**) d- and q-channel of $v_o(t)$

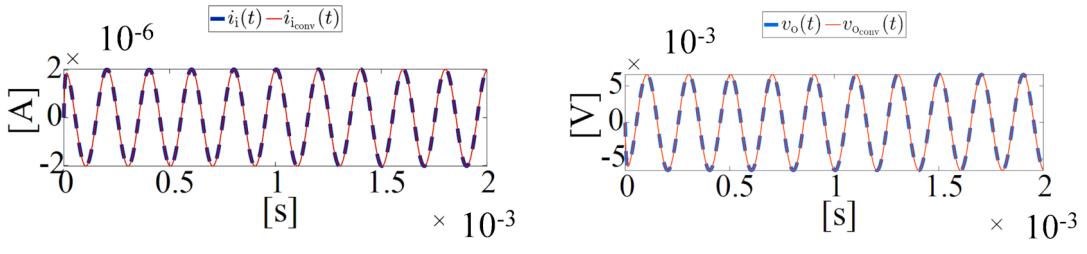

(a) (b)

Figure 9. Simulation results, under transients, show the comparison between the input current and the output voltage derived from the model in (10), i.e., ($i_i(t)$, $v_o(t)$) and those obtained from the inverse conversion of the model in (16) to the model in (10), i.e., ($i_{iconv}(t)$, $v_{oconv}(t)$. (**a**) Comparison between $i_i(t)$, and $i_{iconv}(t)$. (**b**) Comparison between $v_o(t)$, and $v_{oconv}(t)$

Regarding the transformation of the CEA model into d-q coordinates, Figure 8 presents the dynamics of the state variables in the d-q frame. Figure 8a depicts the dynamics of $i_{id}(t)$ and $i_{iq}(t)$, while Figure 8b shows the dynamics of $v_{od}(t)$ and $v_{oq}(t)$. The results in Figure 8 clearly indicate the static nature of the model in d-q coordinates, where the state

variables reach their steady-state values very rapidly (approximately 2 μs) after system start-up. This rapid convergence to steady-state highlights the advantage of the d-q transformation in accelerating the system's response, facilitating a faster transition to the steady-state regime compared to the system described in normal coordinates. Moreover, the dynamics are confirmed as detailed in (53), with Figure 8 illustrating that the steady-state components are indeed constant, as anticipated from the dynamics converted to d-q coordinates.

In Figure 9, the proper operation of the model in d-q coordinates, as presented in (16), is clearly illustrated. The simulation results demonstrate that the pairs of variables $i_i(t)$, $i_{iconv}(t)$ and $v_o(t)$, $v_{oconv}(t)$ exhibit identical dynamics, validating the accuracy and correctness of the CEA's d-q model. This model not only simplifies the analysis of dynamic variables, where their behavior is represented as dc components, but also allows for the potential use of standard linear compensators in control system design, leveraging the simplicity introduced by the d-q transformation.

8. Conclusions

This study delves into the field of microelectronics, with a particular focus on low-power signal amplification. The focus is on the central role that bipolar junction transistors and operational amplifiers play in this context. Operational amplifiers are considered highly versatile across various frequency spectra, whereas bipolar junction transistors face challenges, especially in mid-frequency voltage amplification, due to their gain dependence on the load resistance. To address these challenges, a feedback loop inspired by control theory is introduced, emphasizing the critical role of selecting appropriate actuators and compensators.

A novel common-emitter amplifier model is central, introducing variables with static dynamics. This article meticulously analyzes state equations, unraveling dynamic interactions of state variables in both electrical and d-q coordinates. The analysis examines both transient and steady-state dynamics, providing insight into the vulnerability of sinusoidal and transient components to external factors.

The proposed d-q coordinate model has been rigorously validated through inverse transformations and simulations, confirming its accuracy and reliability. Simulations provide evidence of the model's viability and effectiveness, offering nuanced insights into common-emitter amplifier performance under various scenarios and operating conditions. The transformation to d-q coordinates proves advantageous by allowing the system to reach its steady-state regime more rapidly compared to traditional normal coordinate systems. Additionally, the d-q model facilitates easier analysis of dynamic variables due to their dc behavior, enabling straightforward implementation of conventional linear compensators in control system design.

Conflict of interest

The authors declare that there are no conflict of interest.

References

[1] B. Perez-Verdu, J. L. Huertas, and A. Rodriguez-Vazquez, "A New Nonlinear Time-Domain Op-Amp Macromodel Using Threshold Functions and Digitally Controlled Network Elements," *IEEE J. Solid-State Circ.*, vol. 23, pp. 959–971, 1988, doi:10.1109/4.347.

[2] D. F. Bowers, "A Fast Precision Operational Amplifier Featuring Two Separate Control Loops," in *Proc. 2014 IEEE Bipolar/BiCMOS Circ. Technol. Meeting (BCTM)*, Coronado, CA, USA, Sept. 28–Oct. 1, 2014, pp. 72–75.

[3] M. Gilasgar, A. Barlabé, and L. Pradell, "High-Efficiency Reconfigurable Dual-Band Class-F Power Amplifier With Harmonic Control Network Using MEMS," *IEEE Microw. Wirel. Compon. Lett.*, vol. 30, pp. 677–680, 2020, doi:10.1109/LMWC.2020.2994373.

[4] S. E. Hosseini and H. G. Dehrizi, "A New BJT-Transistor with Ability of Controlling Current Gain," in *Proc. Int. Multi-Conf. Syst., Signals Dev.*, Chemnitz, Germany, Mar. 20–23, 2012, pp. 1–4.

[5] K.-J. De Langen and J. H. Huijsing, "Compact Low-Voltage Power-Efficient Operational Amplifier Cells for VLSI," *IEEE J. Solid-State Circ.*, vol. 33, pp. 1482–1496, 1998, doi:10.1109/4.720394.

[6] L. Kong, et al., "Design of a Wideband Variable-Gain Amplifier With Self-Compensated Transistor for Accurate dB-Linear Characteristic in 65 nm CMOS Technology," *IEEE Trans. Circ. Syst. I Reg. Pap.*, vol. 67, pp. 4187–4198, 2020, doi:10.1109/TCSI.2020.2995725.

[7] I. M. Pandiev and E. C. Stoimenov, "Development of Single-Transistor Amplifier Modular Laboratory Kits for Electronic Engineering Education," in *Proc. 2020 XI Nat. Conf. Int. Particip. (ELECTRONICA)*, Sofia, Bulgaria, Jul. 23–24, 2020, pp. 1–4.

[8] F. A. Farag and Y. A. Khalaf, "Digitally-Controlled Variable-Gain-Amplifier Based on Current Conveyor with Opamp and Inverters Only," in *Proc. 2010 Int. Conf. Microelectron.*, Cairo, Egypt, Dec. 19–22, 2010, pp. 224–227.

[9] D. G. Makarov, V. V. Kryzhanovskyi, V. G. Krizhanovski, and A. V. Grebennikov, "Experimental Investigation of Class E Power Amplifier with Shunt Filter for Reduced Duty Ratio," in *Proc. 2018 Int. Conf. Inform. Telecommun. Technol. Radio Electron. (UkrMiCo)*, Odessa, Ukraine, Sept. 10–14, 2018, pp. 1–4.

[10] Y. Hou, et al., "A 56–161 GHz Common-Emitter Amplifier with 16.5 dB Gain Based on InP DHBT Process," *Electronics*, vol. 10, p. 1654, 2021, doi:10.3390/electronics10141654.

[11] H. Nam, D.-A. Nguyen, Y. Kim, and C. Seo, "Design of 6 GHz Variable-Gain Low-Noise Amplifier Using Adaptive Bias Circuit for Radar Receiver Front End," *Electronics*, vol. 12, p. 2036, 2023, doi:10.3390/electronics12092036.

[12] D. L. Rode, "Output Resistance of the Common-Emitter Amplifier," *IEEE Trans. Electron. Dev.*, vol. 52, pp. 2004–2008, 2005, doi:10.1109/TED.2005.854277.

[13] P. Sivonen, S. Kangasmaa, and A. Parssinen, "Analysis of Packaging Effects and Optimization in Inductively Degenerated Common-Emitter Low-Noise Amplifiers," *IEEE Trans. Microw. Theory Techn.*, vol. 51, pp. 1220–1226, 2003, doi:10.1109/TMTT.2003.809633.

[14] E. Ozeren, C. Cahskan, M. Davulcu, H. Kayahan, and Y. Gurbuz, "4-Bit SiGe Phase Shifter Using Distributed Active Switches and Variable Gain Amplifier for X-Band Phased Array Applications," in *Proc. 2014 9th Eur. Microw. Integr. Circ. Conf.*, Rome, Italy, Oct. 6–7, 2014, pp. 257–260.

[15] J.-Y. Um, "A Compact Variable Gain Amplifier With Continuous Time-Gain Compensation Using Systematic Predistorted Gain Control," *IEEE Trans. Circ. Syst. II*, vol. 69, pp. 274–278, 2022, doi:10.1109/TCSII.2021.3090424.

[16] R. W. Erickson and D. Maksimovic, *Fundamentals of Power Electronics*. Norwell, Mass: Springer Science & Business Media, 2001, ISBN 978-0-7923-7270-7.

[17] C. J. Savant, M. S. Roden, and G. L. Carpenter, *Electronic Design: Circuits and Systems*, Subsequent edition. Redwood City, CA, USA: Benjamin-Cummings Pub Co., 1990, ISBN 978-0-8053-0285-1.

[18] A. S. Sedra and K. C. Smith, *Microelectronic Circuits*. Oxford, UK: Oxford University Press, 2004, ISBN 978-0-19-514252-5.

[19] K. Katsuhiko, *Modern Control Engineering*. Boston, UK: CRC Press, 2009, ISBN 978-0-13-615673-4.

[20] *The Control Handbook (Three Volume Set)*. Boston, UK: CRC Press, 2018, ISBN 978-1-315-21869-4.

[21] B. C. Kuo, *Automatic Control Systems*, 6th ed. Englewood Cliffs, NJ, USA: Prentice Hall, 1991, ISBN 978-0-13-051046-4.

[22] C. J. O' Rourke, M. M. Qasim, M. R. Overlin, and J. L. Kirtley Jr., "A Geometric Interpretation of Reference Frames and Transformations: Dq0, Clarke, and Park," *IEEE Trans. Energy Convers.*, vol. 34, no. 4, pp. 2070–2083, 2019, doi:10.1109/TEC.2019.2941175.

[23] P. Dorato, C. T. Abdallah, and V. Cerone, *Linear Quadratic Control: An Introduction*. Melbourne, FL, USA: Krieger Pub Co., 2000, ISBN 978-1-57524-156-2.

[24] C. J. Savant, M. S. Roden, and G. L. Carpenter, *Electronic Design: Circuits and Systems*, Subsequent ed. Redwood City, CA, USA: Benjamin-Cummings Pub Co, 1990, ISBN 978-0-8053-0285-1.

[25] W. L. Brogan, *Modern Control Theory*. Englewood Cliffs, NJ, USA: Prentice Hall, 1991, ISBN 978-0-13-589763-8.

[26] M. Gonzalez, V. Cardenas, and F. Pazos, "DQ Transformation Development for Single-Phase Systems to Compensate Harmonic Distortion and Reactive Power," in *Proc. 9th IEEE Int. Power Electron. Congr. (CIEP)*, Celaya, Mexico, Oct. 17–22, 2004, pp. 177–182.

[27] M. F. Schonardie and D. C. Martins, "Application of the Dq0 Transformation in the Three-Phase Grid-Connected PV Systems with Active and Reactive Power Control," in *Proc. 2008 IEEE Int. Conf. Sustain. Energy Technol.*, Singapore, Nov. 24–27, 2008, pp. 18–23.

[28] K. S. Low, M. F. Rahman, and K. W. Lim, "The Dq Transformation and Feedback Linearization of a Permanent Magnet Synchronous Motor," in *Proc. 1995 Int. Conf. Power Electron. Drive Syst. (PEDS)*, Singapore, Feb. 21–24, 1995, pp. 292–296, vol. 1.

[29] S. W. L. Tobing, R. Afdila, P. E. Panjaitan, N. C. Situmeang, K. N. Hutagalung, and R. Sidabutar, "ABC to DQ Transformation for Three-Phase Inverter Design as Prime Mover Speed Control in Microgrid System," in *Proc. 2022 6th Int. Conf. Electr. Telecommun. Comput. Eng. (ELTICOM)*, Medan, Indonesia, Nov. 22–23, 2022, pp. 70–74.

[30] M. F. Schonardie, R. F. Coelho, R. Schweitzer, and D. C. Martins, "Control of the Active and Reactive Power Using Dq0 Transformation in a Three-Phase Grid-Connected PV System," in *Proc. 2012 IEEE Int. Symp. Ind. Electron.*, Hangzhou, China, May 28–31, 2012, pp. 264–269.

[31] K. Abe, "The Clark and Park Transformations: Coordinate Transformations for Brushless DC Motor in Field-Oriented Control," Nov. 21, 2017.

[32] B. C. Trento, "Modeling and Control of Single Phase Grid-Tie Converters," M.S. thesis, Univ. Tenn., Knoxville, TN, USA, 2012.

[33] M. R. Spiegel, *Applied Differential Equations*. Upper Saddle River, NJ, USA: Prentice-Hall, 1958.

[34] F. Ayres, *Schaum's Outline of Theory and Problems of Differential Equations*, New York, NY, USA: McGraw-Hill, 1967, ISBN 978-0-07-002654-4.